

Probing two Universal Extra Dimensions at International Linear Collider

Kirtiman Ghosh ^a, Anindya Datta ^b

*Department of Physics, University of Calcutta,
92, A. P. C. Road, Kolkata 700009, India*

ABSTRACT

We discuss collider signatures of $(1, 1)$ -th Kaluza-Klein (KK) mode vector bosons in the framework of *two universal extra dimension model*, at a future e^+e^- collider. Production of $B_\mu^{(1,1)}$ and $W_{3\mu}^{(1,1)}$, the $(1, 1)$ -th KK mode vector bosons, are considered in association with a hard photon. Without caring about the decay products of $B_\mu^{(1,1)}$ or $W_{3\mu}^{(1,1)}$, one can measure the masses of these particles just by looking at the photon energy distribution. Once produced $B_\mu^{(1,1)}$ ($W_{3\mu}^{(1,1)}$) dominantly decays to a pair of jets or to a pair of top quarks. Thus we look for a pair of jets or a pair of top quarks in association with a photon. Upto the kinematic limit (with e^+e^- center-of-mass energies of 0.5 TeV and 1 TeV) of the collider, signals from the $B_\mu^{(1,1)}$ production and decay in both the above mentioned channels are greater than the 5σ fluctuation of the Standard Model background with 500 fb^{-1} integrated luminosity. However, the number of events from $W_{3\mu}^{(1,1)}$ production and decay is smaller and its detection prospect is not very good.

1 Introduction

Recently lots of attention have been paid to the models of fundamental interactions with one or more extra space like dimensions [1, 2]. There is a class of such interesting models where all the Standard Model (SM) fields can access these extra space-like dimensions along with the $(3+1)$ dimensional Minkowski space time. These are collectively called the Universal Extra Dimensional (UED) models [3].

A particular variant of the UED model where all the SM fields propagate in $(5 + 1)$ dimensional space time, namely the *two Universal Extra Dimension* (2UED) Model has some attractive features. 2UED model can naturally explain the long life time for proton decay [4] and more interestingly it predicts that the number of fermion generations should be an integral multiple of three [5].

As the name suggests, in 2UED, all the SM fields can propagate universally in the six-dimensional (6D) space-time. Four dimensional (4D) space time coordinates x^μ ($\mu = 0, 1, 2, 3$) form the usual Minkowski space. Two extra spacial dimensions with coordinates

^aE-mail address: kirtiman.ghosh@saha.ac.in

^b E-mail address: adphys@caluniv.ac.in

x^4 and x^5 are flat and are compactified with $0 \leq x^4, x^5 \leq L$. Toroidal compactification of the extra dimensions, leads to 4D fermions that are vector-like with respect to any gauge symmetry. Alternatively, one needs to identify two pairs of adjacent sides of the square. This compactification mechanism automatically leaves at most a single 4D fermion of definite chirality as the zero mode of any chiral 6D fermion [6].

The requirements of anomaly cancellation and fermion mass generation force the weak-doublet fermions to have opposite *6D chiralities* with respect to the weak-singlet fermions. So the quarks of one generation are given by $Q_+ \equiv (U_+, D_+)$, U_- , D_- . The 6D doublet quarks and leptons decompose into Kaluza-Klein (KK) towers of heavy vector-like 4D fermion doublets with left-handed zero mode doublets. Similarly each 6D singlet quark and lepton decompose into the KK-towers of heavy 4D vector-like singlet fermions along with zero mode right-handed singlets. These zero mode fields are identified with the SM fermions. In 6D, each of the gauge fields, has six components. Upon compactification, they give rise to towers of physical 4D massive spin-1 fields and a tower of spinless adjoints. In a previous work [7] we have discussed the phenomenology of these spinless adjoints in some details. In this letter, we will be interested in a particular member of the KK-towers of hypercharge gauge boson B_μ and $SU(2)$ gauge boson W_μ^3 .

We would like to investigate the production of B_μ and W_μ^3 in association with a *hard* photon at a future e^+e^- linear collider. Somewhat similar things have been discussed in Ref. [8]. Authors in Ref. [8], have considered the production of B_μ in association with a photon. However, they demand that the photon is undetectable and is lost along the beam pipe. This implies that the identification and mass determination of B_μ , crucially depend on jet (coming from the decay of B_μ) reconstruction and jet energy measurement. In contrast, we look for a final state consisting of a *hard* photon and the decay products (which may or may not be detectable always) of B_μ and W_μ^3 . In some sense our method is complementary to that used in Ref. [8]. The advantages of tagging the photon, will be illuminated in the next section.

The tree-level masses for $(j, k)^3$ -th KK-mode particles are given by $\sqrt{M_{j,k}^2 + m_0^2}$, where $M_{j,k} = \sqrt{j^2 + k^2}/R$. The radius of compactification, R , is related to the size of the extra dimensions, L via the relation $L = \pi R$. m_0 is the mass of the corresponding zero mode particle. As a result, the tree-level masses are approximately degenerate. This degeneracy is lifted by radiative corrections.

Conservation of momentum (along the extra dimensions) in the full theory, implies KK number conservation in the effective 4D theory. SM-like interactions in the 6D, (called the *bulk interactions*) give rise to the *KK-number conserving* as well as *KK-parity conserving* interactions, in 4D effective theory after compactification. However, one can generate KK number violating (KK parity conserving) operators at one loop level, starting from the bulk interactions. Structure of the theory demands that these operators can only be on $(0, 0)$, $(0, L)$ and (L, L) points of the *chiral square*. In this letter, we will exploit one such KK-number violating coupling to find a characteristic signature of 2UED model at an e^+e^- collider. Namely, we will discuss the collider signatures of $B_\mu^{(1,1)}$ and $W_{3\mu}^{(1,1)}$, the $(1, 1)$ -th KK excitations of the $U(1)$ and neutral $SU(2)$ gauge bosons. $B_\mu^{(1,1)}$ ($W_{3\mu}^{(1,1)}$) couples to an electron-positron pair via KK-number violating coupling [9]:

$$\mathcal{L} = [\bar{e} (c_L^V P_L + c_R^V P_R) \gamma^\mu e] V_\mu^{(1,1)}. \quad (1)$$

³Each member of a KK-tower is specified by a pair of integers, called the KK-numbers.

Where,

$$\begin{aligned}
c_L^B &= \frac{g'g^2}{16\pi^2} \left(\frac{9}{8} + \frac{91}{24} \frac{g'^2}{g^2} \right) \ln \frac{M_s^2}{M_{j,k}^2}, \\
c_R^B &= \frac{g'^3}{16\pi^2} \left(\frac{59}{6} \right) \ln \frac{M_s^2}{M_{j,k}^2}, \\
c_L^{W^3} &= \frac{g^3}{16\pi^2} \left(-\frac{11}{24} + \frac{3g'^2}{8g^2} \right) \ln \frac{M_s^2}{M_{j,k}^2}, \\
c_R^{W^3} &= 0.
\end{aligned} \tag{2}$$

These couplings also have logarithmic dependence on the cutoff scale, M_s , of the theory. We assume M_s to be 10 times the compactification scale R^{-1} following [9].

Contributions to the KK-number violating operators like Eq. (1) might be induced by physics above the cut-off scale. We assume that those UV generated localized operators are also symmetric under KK parity, so that the stability of the lightest KK particle which can be a promising dark matter candidate [11], is ensured. Loop contributions by the physics below cut-off scale M_s are used to renormalize the localized operators [12].

2 Signatures at future e^+e^- collider with photon tag

Resonance production of $B_\mu^{(1,1)}$, has been investigated in the context of Tevatron and LHC in [9, 10] and in the context of future e^+e^- collider in [8]. However, in this letter, we will reconsider the prospects of $B_\mu^{(1,1)}$ (also $W_{3\mu}^{(1,1)}$) production and detection at future e^+e^- colliders, exploiting the KK-number violating couplings defined in Eq. (1).

There is a disadvantage of e^+e^- collision. Unless the mass of the particle, we want to produce, matches exactly with the e^+e^- center-of-mass energy, resonance production cross-section is miniscule. This compels us to consider the $B_\mu^{(1,1)}$ ($W_{3\mu}^{(1,1)}$) production in association with a photon ($e^+e^- \rightarrow \gamma B_\mu^{(1,1)}, \gamma W_{3\mu}^{(1,1)}$). This particular production mechanism has many interesting consequences. First of all, just measuring the photon energy one can have the knowledge of the mass of $B_\mu^{(1,1)}$, without caring about the decay products of $B_\mu^{(1,1)}$. Moreover, we will also notice that, the production cross-section grows with mass of $B_\mu^{(1,1)}$ ($W_{3\mu}^{(1,1)}$).

$B_\mu^{(1,1)}$ and $W_{3\mu}^{(1,1)}$ production in association with a photon takes place in e^+e^- collision, via t(u) channel. Spin averaged matrix element squared at the LO is given by :

$$\overline{\sum |\mathcal{M}|^2} = 4\pi\alpha_{em} (c_L^{V^2} + c_R^{V^2}) \left(\frac{u}{t} + \frac{t}{u} + \frac{2m_V^2 s}{ut} \right), \tag{3}$$

s, t, u are the usual Mandelstam variables, and c_L^V , c_R^V are defined in Eq. (2). The numerical values of the cross-sections are presented in Fig. 1 against the masses of $B_\mu^{(1,1)}$ and $W_{3\mu}^{(1,1)}$ for two different values of e^+e^- center-of-mass energies. Fig. 1 shows a very interesting variation of cross-section. In spite of the fact that, the couplings in Eq. (1) do not increase with the masses or R^{-1} , the cross-section increases when the mass of $V_\mu^{(1,1)}$ approaches closer to the center-of-mass energy, which is fixed for a particular collider. This, in fact, is a more general phenomena not specific to the 2-UED model. The probability of the photon emission from one of the initial e^- or e^+ , increases with the diminishing photon energy. One can easily

check that for a fixed center-of-mass energy (\sqrt{s}) of the collider, photon energy E_γ is given by: $\frac{s-m^2}{2\sqrt{s}}$. Thus a KK gauge boson mass closer to the center-of-mass energy reduces the photon energy which in turn increases the cross-section. Similar effects can take place in the cases of single production of sneutrinos [13] (in association with a photon) via lepton number violating couplings; graviton production in ADD or RS model (in association with a photon) [14].

The increase of cross-section with mass can also be very easily understood by looking at Eq. (3). Both, u and t are proportional to the photon energy E_γ . An increasing $B_\mu^{(1,1)}$ or $W_{3\mu}^{(1,1)}$ mass would mean (for a fixed e^+e^- center-of-mass energy) a diminishing u and t . This in turn enhances the cross-section with mass.

Rate of $B_\mu^{(1,1)}$ production is always an order of magnitude higher than the rate of $W_{3\mu}^{(1,1)}$ production over the mass range upto the kinematic limit. $W_{3\mu}^{(1,1)}$ couples only to the left-handed electrons via the $SU(2)$ gauge coupling. On the other hand, $B_\mu^{(1,1)}$ couples to both left- and the right-handed electrons (see Eq. (2)). Moreover, a partial cancellation between two terms in the expression of $c_L^{W^3}$ makes the $W_{3\mu}^{(1,1)}$ production cross-section smaller. The dominance of $B_\mu^{(1,1)}$ cross-section over the $W_{3\mu}^{(1,1)}$ can be partially explained from these couplings.

We can now discuss the signals of $B_\mu^{(1,1)}$ and $W_{3\mu}^{(1,1)}$ production at e^+e^- collisions. Once produced, $B_\mu^{(1,1)}$ ($W_{3\mu}^{(1,1)}$) dominantly decays to a pair of light quark jets. It also decays to a $b\bar{b}$ or $t\bar{t}$ pair. We collectively look for two jets (light or b -flavoured) from the decay of $B_\mu^{(1,1)}$ or $W_{3\mu}^{(1,1)}$ and a nearly mono-energetic photon. If we look at the energy distribution of the photons, $B_\mu^{(1,1)}$ and $W_{3\mu}^{(1,1)}$ production would be characterised by two (mono-energetic) peaks separated by, $\Delta E_\gamma = \frac{m_{W_{3\mu}^{(1,1)}}^2 - m_{B_\mu^{(1,1)}}^2}{2\sqrt{s}}$.

Production of $B_\mu^{(1,1)}$ ($W_{3\mu}^{(1,1)}$), in association with a photon, is twofold advantageous. Instead of a fixed center-of-mass energy, now the effective center-of-mass energy of the collision (which produces the new physics) can vary over a range thus makes it possible to produce $B_\mu^{(1,1)}$ and/or $W_{3\mu}^{(1,1)}$ with different masses. Moreover, by measuring the energy of the photon, we can determine the masses of $B_\mu^{(1,1)}$ and $W_{3\mu}^{(1,1)}$ without caring about the decays of these particles⁴. $B_\mu^{(1,1)}$ or $W_{3\mu}^{(1,1)}$ dominantly decays to a pair of jets. One can thus measure the masses of $B_\mu^{(1,1)}$ or $W_{3\mu}^{(1,1)}$, directly by measuring the jet energies. Authors in Ref. [8], have investigated the production of $B_\mu^{(1,1)}$ in e^+e^- collision. They have emphasised on directly measuring the jet energies and reconstructing the $B_\mu^{(1,1)}$ mass. This involves, identification and energy measurement of *both* the jets coming from the $B_\mu^{(1,1)}$ decay. However, photon identification and measurement of its energy in electromagnetic calorimeter can be done more easily in comparison to the same exercise with the jets.

For an ideal detector with infinitely high resolution, the photon energy distribution is ideally an delta-function at $E_\gamma = \frac{s-m_{B_\mu}^2}{2\sqrt{s}}$. As a consequence of finite detector resolution and initial state radiation (ISR) the photon energy distribution is smeared. However, the effects which smear the E_γ peak, cannot change the position of the peak, enabling us to measure the masses of $B_\mu^{(1,1)}$ or $W_{3\mu}^{(1,1)}$ just by looking at the position of the peaks in the E_γ

⁴ Similar technique has been exploited in [15] to find the signals of doubly-charged Higgs at an e^-e^- collider.

distribution. This method works well, independent of any particular decay mode of $B_\mu^{(1,1)}$ ($W_{3\mu}^{(1,1)}$). As for example, one can consider the case of $B_\mu^{(1,1)}$ decaying to $t\bar{t}$ (branching ratio of $B_\mu^{(1,1)}(W_{3\mu}^{(1,1)}) \rightarrow t\bar{t}$ is 30 (15) %). Final state comprises of missing energy/momentum due to the presence of neutrinos if one allows the top quarks to decay semi-leptonically. In such a situation, reconstructing the $B_\mu^{(1,1)}$ mass will be difficult. Even when the top quarks decay hadronically, we have to be careful about reconstructing the two top quarks out of the six jets. This would be a challenging task. However, just by looking at the nearly mono-energetic photon, we ease our task by a considerable amount.

We have also estimated the SM contribution to the $\gamma + 2j$ final state. Fig. 2 shows the E_γ distributions for signal (dashed histogram) and background (solid histogram) for an e^+e^- center-of-mass energy of 1 TeV. We have used $R^{-1} = 630$ GeV for the purpose of illustration in this figure. ISR effects have been included in our analysis following the prescription in Ref. [16]. To include a realistic detector response, we have smeared the photon and jet momenta using a Gaussian smearing [17]. The topology of signal and background events are more or less the same. As a result, the kinematic cuts defined below are for the purpose of selection only.

The following selection criteria are applied on signal and backgrounds:

$$p_T^\gamma > 10 \text{ GeV}, p_T^j > 20 \text{ GeV},$$

$$|\eta_\gamma| < 2.5, |\eta_j| < 3,$$

$$\Delta R \left(\equiv \sqrt{\Delta\eta^2 + \Delta\phi^2} \right) \text{ (between any pair of photon and jets)} > 0.7.$$

e^+e^- C-o-M Energy	R^{-1} in GeV	$B_\mu^{(1,1)}$			$W_\mu^{3(1,1)}$		
		$m_{B_\mu^{(1,1)}}$ GeV	Signal Event	Background Event	$m_{W_\mu^{3(1,1)}}$ GeV	Signal Event	Background Event
500 GeV	280	387.3	5900	19258 (139)	433.8	253	26593 (163)
	290	401.1	6713	20368 (143)	448.7	349	34031 (184)
	300	414.9	7701	22207 (149)	463.7	520	50011 (224)
	310	428.8	9005	24814 (158)	478.7	-	-
	340	470.3	24296	59938 (245)	523.6	-	-
1 TeV	300	414.9	348	2889 (54)	463.7	10	2499 (50)
	400	553.3	430	2038 (45)	613.8	14	1932 (44)
	550	760.8	948	2096 (46)	840.4	43	2538 (50)
	630	871.4	2082	3013 (55)	961.5	210	8444 (92)
	690	954.4	6552	7482 (87)	1052.4	-	-

Table 1: Number of $\gamma + 2j$ signal and SM background events for two values of e^+e^- center-of-mass energies assuming 500 fb^{-1} integrated luminosity. 1σ fluctuations of the background events are also shown in the brackets. The entries marked with a dash, correspond to the situations when number of events are too small, or $B_\mu^{(1,1)}$ ($W_{3\mu}^{(1,1)}$) production is kinematically disallowed.

In Table 1, the total number of signal events in the bins corresponding to the peak in the photon energy distributions and its two adjacent bins are presented for different values of R^{-1} . We have used a bin size of 5 GeV. The total number of background events corresponding to the above three bins are also presented with their 1σ fluctuations. It is

evident from the table, almost upto the kinematic limit of the e^+e^- collision, signal from $B_\mu^{(1,1)}$ is always greater than the 5σ fluctuation of the background. However, the signal from $W_{3\mu}^{(1,1)}$ is weaker and merely can surpass the 1σ fluctuation of the SM background for $W_{3\mu}^{(1,1)}$ masses closer to the e^+e^- center-of-mass energy. Thus it is not possible to measure both the peaks over the SM background. This in turn kills the hope to measure the correlation between the masses and the cross-sections of the $W_{3\mu}^{(1,1)}$ and $B_\mu^{(1,1)}$ production in 2UED.

Now we will discuss the situation when $B_\mu^{(1,1)}$ or $W_{3\mu}^{(1,1)}$ decays to $t\bar{t}$. Final state thus consists of a monoenergetic photon with decay products coming from the pair of top quarks. Instead of incorporating the detailed decay and reconstruction of top quarks at the detector level, we have multiplied our cross-sections by top reconstruction efficiency (0.55) in 6-jet and 4-jet plus 1-lepton channel [18] in our analysis. In Table 2, the numbers of $\gamma + 2t$ events corresponding to the bin (and its two adjacent bins) for which E_γ distributions shows the characteristic peak, are presented for signal and background. Number of $2t$ events from $B_\mu^{(1,1)}$ are smaller with respect to the $2j$ events, due to smaller branching ratio and top-reconstruction efficiency. Number of background events are also smaller in $2t$ channel compared to the $2j$ channel.

Number of events from the $B_\mu^{(1,1)}$ production and decay (either in $2j$ or $2t$ mode) are always well above the 5σ fluctuations of the SM background. This opens up a possibility, to measure cleanly the relative strengths of the signals from $B_\mu^{(1,1)}$ decaying into $2j$ and $2t$ channels⁵. Consequently one can determine the *ratios of the decay widths* of $B_\mu^{(1,1)}$ into jj mode and $t\bar{t}$ mode. This ratio is *not sensitive* to the cut-off scale M_s unlike the cross-sections. Apart from the coupling constants, the ratio depends only on $B_\mu^{(1,1)}$ mass (not on other parameters like R or M_s). Mass of $B_\mu^{(1,1)}$ also can be measured independently from the peak position of E_γ distribution. Using this value of experimentally measured mass, one can calculate the ratio as in the 2UED model. Finally, this theoretical number can be compared with the experimentally measured ratio of decay widths.

Number of $\gamma + 2t$ events from $W_{3\mu}^{(1,1)}$ production is again small and cannot compete with the SM background. For the sake of completeness, we have presented these numbers also in Table 2.

3 Conclusion

To summarise, we have discussed a possible signature of $B_\mu^{(1,1)}$ and $W_{3\mu}^{(1,1)}$ production along with a hard photon, in the framework of 2UED model, at a future e^+e^- collider. Once produced these gauge bosons decay either to a pair of light quarks or to a pair of top quarks. So the signatures of these vector bosons are a pair of jets or a pair of top quarks with a nearly monoenergetic photon. Production of these (1,1)-mode gauge bosons along with a single hard photon is advantageous. Without caring about the decay products of $B_\mu^{(1,1)}$ and $W_{3\mu}^{(1,1)}$, one can measure the masses of these particles by measuring the energy of the photon. Number of signal events from $B_\mu^{(1,1)}$ production is always greater than the 5σ fluctuation of the SM background, for R^{-1} values up to the kinematic limit of the collision. Rate of $W_{3\mu}^{(1,1)}$ production is small and cannot stand over the SM background in either $2t$ or $2j$ channel. Thus the measurement of the possible correlation between the masses of $B_\mu^{(1,1)}$ and $W_{3\mu}^{(1,1)}$ and

⁵Modulo the detection efficiencies in both these channels, which could be determined beforehand from simulation and experimental data.

e^+e^- C-o-M Energy	R^{-1} in GeV	$B_\mu^{(1,1)}$			$W_\mu^{3(1,1)}$		
		$m_{B_\mu^{(1,1)}}$ GeV	Signal Event	Background Event	$m_{W_\mu^{3(1,1)}}$ GeV	Signal Event	Background Event
500 GeV	250	345.8	-	-	389.1	8	484 (22)
	280	387.3	519	484 (22)	433.8	18	774 (28)
	295	408.1	776	506 (23)	456.2	30	1305 (36)
	310	428.8	1115	711 (27)	478.7	46	1673 (41)
	340	470.3	3586	2248 (48)	523.6	-	-
1 TeV	300	414.9	40	63 (8)	463.7	-	-
	400	553.3	76	77(9)	613.8	-	-
	550	760.8	189	126 (11)	840.4	5	178 (13)
	630	871.4	461	245 (16)	961.5	25	747 (27)
	690	954.4	1482	654 (26)	1052.5	-	-

Table 2: Number of $\gamma + 2t$ signal and SM background events for two values of e^+e^- center-of-mass energies assuming 500 fb^{-1} integrated luminosity. 1σ fluctuations of the background events are also shown in the brackets. The entries marked with a dash, correspond to the situations when number of events are too small, or $B_\mu^{(1,1)}$ ($W_{3\mu}^{(1,1)}$) production is kinematically disallowed or $B_\mu^{(1,1)}$ ($W_{3\mu}^{(1,1)}$) decay to $t\bar{t}$ is kinematically not possible .

their signal strengths is not possible. However, the number of events from $B_\mu^{(1,1)}$ production and decay (both in $\gamma + 2j$ and $\gamma + 2t$ channels) are large. These enable one to measure the cross-sections in these channels precisely. The relative strength of the $\gamma + 2j$ and $\gamma + 2t$ signals thus can be measured. This ratio of the cross-sections are equal to the ratio of $B_\mu^{(1,1)}$ decay widths into jj and $t\bar{t}$ channels. Interestingly this ratio is independent of the cut-off scale of the theory. Thus experimentally measured ratio can be contrasted with the theoretical predictions from 2UED model.

Acknowledgments KG acknowledges the support from Council of Scientific and Industrial Research, Govt. of India. AD is partially supported by Council of Scientific and Industrial Research, Govt. of India, via a research grant 03(1085)/07/EMR-II. AD is also partially supported by DAE-BRNS research grant 2007/37/9/BRNS.

References

- [1] I. Antoniadis, Phys. Lett. B **246**, 377 (1990); N. Arkani-Hamed, S. Dimopoulos and G. Dvali, Phys. Lett. B **429**, 263 (1998); I. Antoniadis, N. Arkani-Hamed, S. Dimopoulos and G. R. Dvali, Phys. Lett. B **436**, 257 (1998).
- [2] L. Randall and R. Sundrum, Phys. Rev. Lett. **83**, 3370 (1999); *ibid* **83**, 4690 (1999).
- [3] T. Appelquist, H. C. Cheng and B. A. Dobrescu, Phys. Rev. D **64**, 035002 (2001); H. C. Cheng, K. T. Matchev and M. Schmaltz, Phys. Rev. D **66**, 056006 (2002).
- [4] T. Appelquist, B. Dobrescu, E. Ponton, H. Yee, Phys. Rev. Lett. **87**, 181802 (2001).

- [5] B. Dobrescu, E. Poppitz, Phys. Rev. Lett. **87**, 031801 (2001).
- [6] B. Dobrescu, E. Ponton, J. High Energy Phys. **071**, 0403, (2004); G. Burdman, B. Dobrescu, E. Ponton, J. High Energy Phys. **33**, 0602, 2006.
- [7] K. Ghosh, A. Datta, Nucl. Phys. **B800**, 109 (2008).
- [8] A. Freitas and K. Kong, JHEP **0802**, 068 (2008).
- [9] G. Burdman, B. Dobrescu, E. Ponton, Phys. Rev. D **74**, 075008 (2006).
- [10] B. Dobrescu, K. Kong, R. Mahbubani, J. High Energy Phys. **006**, 0707, (2007).
- [11] B. Dobrescu, D. Hooper, K. Kong, R. Mahbubani, Jour. Cosmo. Astro. Phys. **0710**, 012 (2007).
- [12] E. Ponton and L. Wang, J. High Energy Phys. **0611**, 018, (2006).
- [13] D. Choudhury, S. K. Rai and S. Raychaudhuri, Phys. Rev. D **71**, 095009 (2005).
- [14] S. K. Rai and S. Raychaudhuri, J. High Energy Phys. **020**, 0310, (2003).
- [15] B. Mukhopadhyaya and S. K. Rai, Phys. Lett. B **633**, 519 (2006).
- [16] E.A. Kuraev, V.S. Fadin, Sov. J. Nucl. Phys. **41** (1985) 466.
- [17] H. Murayama and M. E. Peskin, Ann. Rev. Nucl. Part. Sci. **46**, 533 (1996)
- [18] M. Iwasaki [The Linear Collider Detector Group], arXiv:hep-ex/0102014.

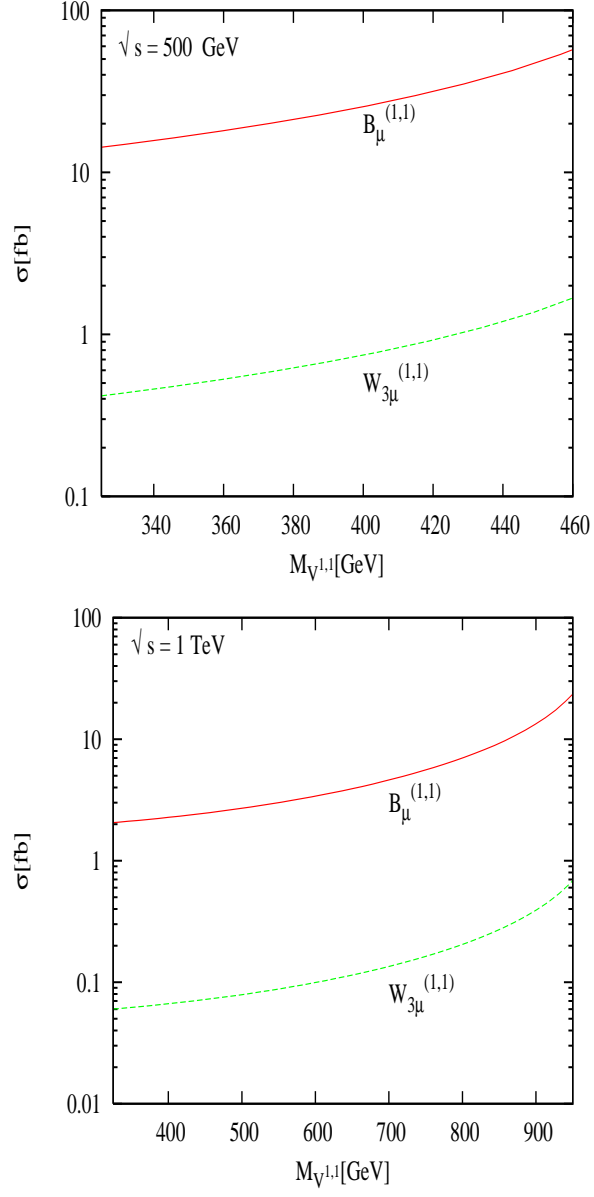


Figure 1: Cross-sections (fb) of $e^+e^- \rightarrow \gamma B_{\mu}^{(1,1)}$ (solidline), $\gamma W_{3\mu}^{(1,1)}$ (dashedline) for e^+e^- center-of-mass energies 0.5, 1 TeV respectively.

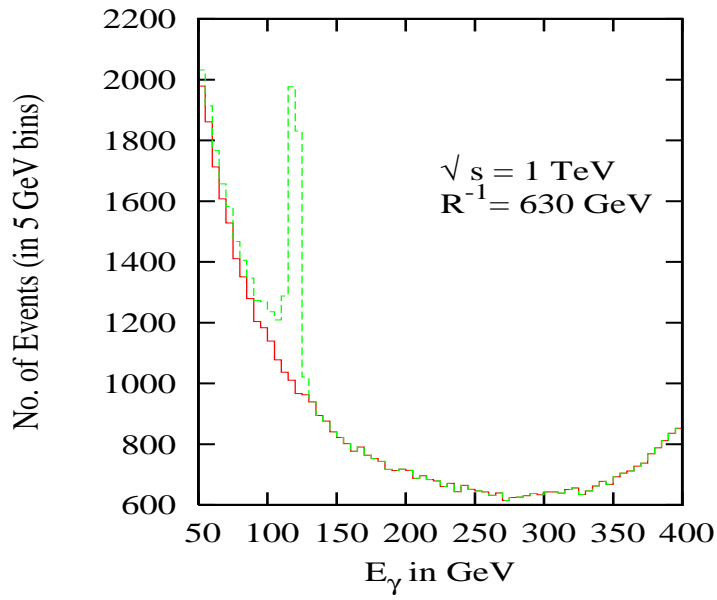


Figure 2: Photon energy distribution for $\gamma + 2j$ -events for signal (dashed histogram) and background (solid histogram). The monoenergetic (in case of the signal) photon peak is smeared due to ISR effects and finite detector resolution. We have used $R^{-1} = 630$ GeV, and $\sqrt{s_{ee}} = 1$ TeV.